The Effect of Molar Weight on Airborne Infectiousness of Coronavirus

N. KHAJOHNSAKSUMETH
Department of Mathematics, Faculty of Science, Mahidol University,
Rama 6 Rd., Bangkok 10400,
THAILAND

also with
Centre of Excellence in Mathematics, MHESI,
Bangkok, 10400,
THAILAND

Abstract: - To design an effective ventilation system in healthcare settings, understanding the ventilation pattern is necessary. In this research, we have investigated the effect of the weight of airborne coronavirus on the spread of the COVID-19 infection. We have mathematically modeled the distribution of the virus as a transport of concentration, including the Navier-Stoke equation and continuity equation. The finite element method was applied to drive the simulations. The numerical results have been obtained and analyzed in this report.

Key-Words: - Air Borne Infection, Mathematical Modelling, Finite Element, COVID-19, Numerical Simulation, SARS-CoV-2, Ventilation Flow, Transmission, Airborne Pathogens.

Received: April 11, 2023. Revised: November 27, 2023. Accepted: January 2, 2024. Published: March 2, 2024.

1 Introduction

In late December 2019, the coronavirus disease (COVID-19), caused by SARS-CoV-2, began to infect the population and spread around the world. By March 2020, there were more than 210000 patients infected with the virus in 168 countries, including nearly 9000 deaths, [1]. Because of the official recognition of its global rapid spread and impact of the virus, COVID-19 was declared a pandemic by the World Health Organization (WHO), [2]. Several researchers have reported on their findings regarding different aspects of the pandemic, [3], [4], [5], [6] and, [7].

COVID-19 is reportedly transmitted through infectious airborne particles and droplets, [8]. Infected persons release respiratory fluids carrying the SARS-CoV-2 virus into the air when they breathe, speak, cough, or sneeze. These particles vary in size, covering a wide range of sizes so that the infection can be easily transmitted from one patient to another. If a susceptible person inhales infectious airborne particles and those particles are lodged in a suitable location within the respiratory tract, that person is at risk of contracting the disease. Particularly in indoor settings such as patients' rooms in hospitals, very fine droplets and particles easily spread through the air throughout the room or living space, [9]. Moreover, droplets remain airborne and allow the virus to accumulate, leading to a higher concentration of infected droplets in the room. When doctors or nurses need to enter the patients' room to follow up the patient's condition, they must practice greater care for themselves; otherwise, they risk easy infection from these droplets or particles. To protect against infection with COVID-19, or any airborne infectious diseases, it is very important to gain more information about the dynamic behavior and characteristics of the spread of the virus.

Many researchers have examined the relationship between ventilation and control of airflow directions in buildings, and the transmission and spread of airborne disease, [8], [10]. Additionally, researchers have studied the effect of saliva and mucus particle size on pathogen generation through the action of breathing, coughing, and sneezing by an infected person, [11], [12]. The majority of human exhaled droplets are within the sub-micrometer size range, [13]. Furthermore, researchers have investigated the evaporation process within indoor environments and the influencing factors, including the ventilation rate, indoor air relative humidity, indoor air temperature, and so on [14], [15], [16], [17].

Recent research, [18], provided valuable insights into the characterization of SARS-CoV-2, enhancing our understanding of COVID-19 and its

behavior. Based on this knowledge, our study focuses on investigating the effect of the weight of airborne infectious particles on dispersion patterns, which, to our knowledge, has not been carried out before. This knowledge is essential for designing the current ventilation systems in healthcare settings effectively.

2 Mathematical Model

To describe the transport of SARS-CoV-2 in a patient's room in a hospital, a transport model for the dynamical system is developed. In what follows, the state variables and parameters are as defined in Table 1. The incompressible laminar airflow and propagation of SARS-CoV-2 in the patients' room region Ω are governed by the following initial boundary value problem (IBVP) in the 3-dimensional - space.

The Navier-Stokes equation (1) along with the continuity equation (2) are applied to describe the movement of fluid in laminar flow. Additionally, in studying gaseous and liquid mixtures, it is necessary to consider the molecular interactions between all species, upon which the properties of mixtures rely. This includes incorporating the transport equation for concentrated species (3).

Laminar Flow

$$\rho(\boldsymbol{u}\cdot\nabla)\boldsymbol{u} = \nabla\cdot\left[-p\boldsymbol{I} + \mu\left(\nabla\boldsymbol{u} + (\nabla\boldsymbol{u})^T\right)\right] + \boldsymbol{F}\,, \quad (1)$$

$$\rho\nabla\cdot\boldsymbol{u} = 0\,. \quad (2)$$

Transport of Concentrated Species

$$\nabla\cdot\boldsymbol{j}_i + \rho(\boldsymbol{u}\cdot\nabla)\omega_i = R_i\,. \quad (3)$$

Based on the relative mass flux due to molecular diffusion using a Fick's law approximation, the diffusive flux can be described as the mixture-averaged diffusion as follows:

$$\boldsymbol{j}_i = -\left(\rho_m D_i^m \nabla\omega_i + \rho\omega_i D_i^m \frac{\nabla M_n}{M_n} - \boldsymbol{j}_{c,i} + D_i^T \frac{\nabla T}{T}\right), \quad (4)$$

where

$$D_i^m = \frac{1-\omega_i}{\sum_{k\neq i}\frac{x_k}{D_{ik}}}\,,\quad M_n = \left(\sum_i \frac{\omega_i}{M_i}\right)^{-1}\,,$$

$$\boldsymbol{j}_{c,i} = \rho\omega_i \sum_k \frac{M_i}{M_n} D_k^m \nabla x_k\,.$$

and ∇ denotes the gradient operator. The subscript i, equaling 1 or 2, corresponds to species 1 or species 2, respectively, for which air is species 1 and infectious particles constitute species 2, and similarly for the subscript k being 1, 2 in the above equations.

Wall Conditions

Under a no-slip condition,

$$u|_{\text{wall}} = 0 \qquad \text{m/s} \qquad (5)$$

Inlet Condition

We apply a normal air inflow velocity for each inlet on the ceiling by

$$u|_{\text{inlet}} = 5 \qquad \text{m/s} \qquad (6)$$

Table 1. Definitions of state variables and parameters in the IBVP described in the text

Variable/ Parameter	Definition
x, y, z	Spatial coordinates
t	Time
$x_k, k = 1,2$	The molar fraction of species k, where k = 1 corresponds to air, and k = 2 corresponds to infectious particles
T	Temperature
$\boldsymbol{u} = \boldsymbol{u}(x, y, z, t)$	velocity vector at (x, y, z, t)
u	The norm of $\boldsymbol{u}$
ρ	Air density
ρ_m	Mixture density
p	Pressure
μ	Dynamic viscosity
$\boldsymbol{F}$	External force
$\boldsymbol{j}_i$	Diffusive flux of species i, where i = 1 corresponds to air, and i = 2 corresponds to infectious particles
R_i	Rate expression describing production or consumption of species i
ω_i	Mass fraction of species i
M_i	The molar mass of species i
M_n	Mean of molar mass
$\boldsymbol{j}_{c,i}$	Relative mass flux of species i
D_{ik}	Multicomponent Fick diffusiveness
ω_i	Mass fraction of species i
$J_{w1,w2}$	Mass flow rate
$\omega_{0,w2}$	Initial value of the mass fraction of infectious particle

Outlet Condition

At the outlet, we assume that the pressure is constant, that is,

$$p|_{\text{outlet}} = 5 \qquad \text{atm} \qquad (7)$$

Boundary Conditions
On the boundary Ω, we define

$$u|_{\partial\Omega} = 5 \quad \text{m/s} \tag{8}$$

Under the no-flux assumption,

$$-\boldsymbol{n}.\boldsymbol{j}_i = 0 \tag{9}$$

The nostril inflow from a patient breathing out is defined as a periodic sine function as follows:

$$J_{wl,w2} = 4\sin(t) + 4 \ \text{kg/s} \tag{10}$$

For the outflow, we assume that

$$-\boldsymbol{n}.\rho D_i^m \nabla \omega_i = 0 \tag{11}$$

Initial Values
Initially, the mass flow rate of infectious particles is

$$\omega_{0,w2} = 0.1 \tag{12}$$

The mixture specification is given in Table 2.

Table 2. Mixture parameter values for coronavirus simulation based on [19], [20], [21]

Parameter	Description and Unit	Value(s)
ρ_m	Mixture density (kg/m^3)	1
M_{w1}	The molar mass of air (kg/mol)	28.9647
M_{w2}	The molar mass of infectious particle (kg/mol)	1 and 5

3 Domains of Computation

In this work, we establish the study scenario in which the patients' room, measuring 10 × 4 × 2.5 meters, is shared by four individuals. The room is equipped with a closed door measuring 1 × 2 meters, four air inlets on the ceiling at the end of the bed, each measuring 0.5 × 0.5 meters, and four outlets on the wall above each patient's head, each measuring 0.25 × 0.25 meters, designed to release airborne pathogens from the room.

Moreover, each patient is provided a bed partition to separate them individually, and the nostril is designed on each patient's head to release the mixture of fluid flow inlet containing infectious droplets, as shown in Figure 1 (a).

In Figure 1 (b), the meshing of the computational domain, necessary for the application of the finite element approach, is shown. In addition, the locations where data points for collecting computational values from the finite element analysis are situated and labeled as points A, B, C, D, and E, respectively, may be seen in Figure 2 and Figure 3.

Point A is situated above the leftmost patient's breast as shown in Figure 2 (a). Point B is positioned above the leftmost patient's feet as shown in Figure 2 (b). Point C is located below, near the outlet flow of the leftmost patient as shown in Figure 3 (a). Point D is placed at the door to determine if a doctor or nurse enters the room as shown in Figure 3 (b). Lastly, point E is placed at the inlet flow of the second leftmost patient in the room as shown in Figure 3 (c).

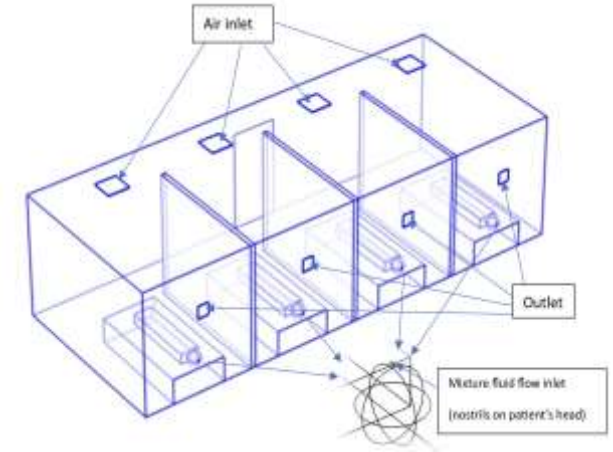

(a)

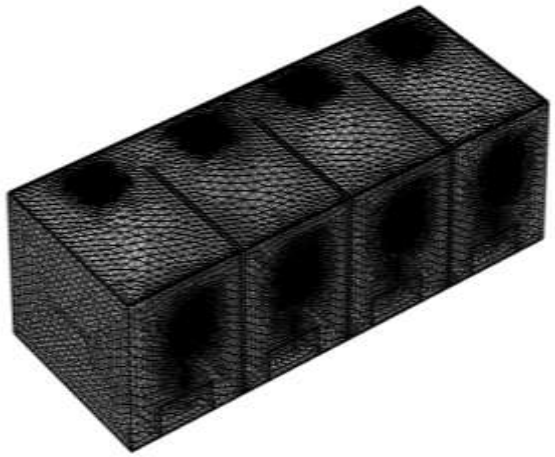

(b)

Fig. 1: Domain of computation: (a) computational domain, showing the locations of flow inlets and outlets, and (b) meshing domain. In (a), the patient's head has been enlarged to show the position of the patient's nostrils which is the flow inlet of the mixture fluid

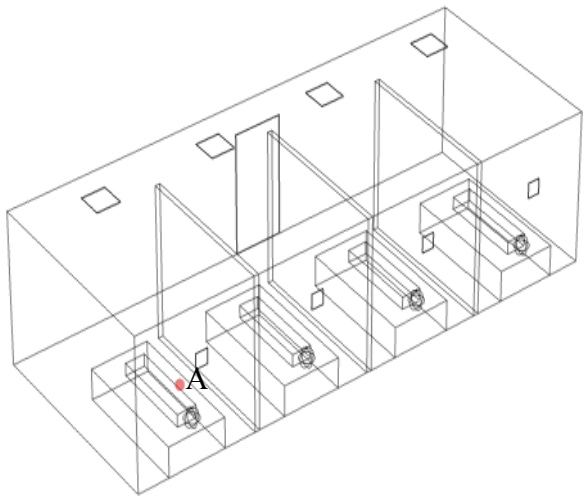

(a)

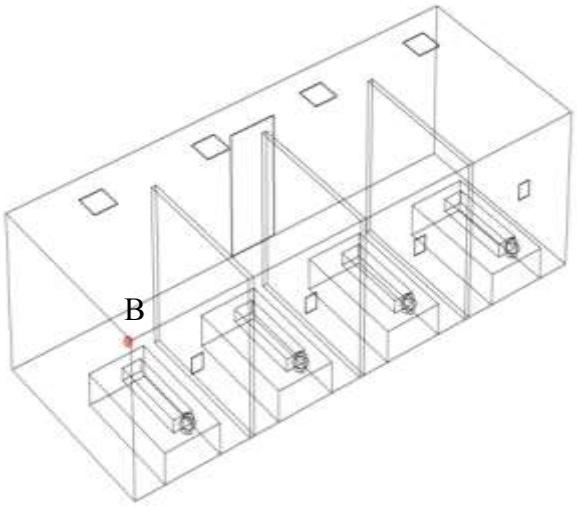

(b)

Fig. 2: Locations of points, in red, for collected computation values labeled as (a) point A, and (b) point B.

4 Numerical Results and Discussion

In this section, the influence of the molar mass of airborne pathogens on the molar concentration of air and airborne pathogens at various locations in the patients' room is numerically investigated. In Figure 4, Figure 5, Figure 6, Figure 7 and Figure 8 the numerical results are displayed for a scenario in which the molar mass of airborne pathogens is 1 kg/mol.

Here, the concentrations of both air and airborne pathogens at five different locations are presented. We observe that at point A, located near the inflow of airborne pathogens, the air concentration is very low to begin with, while the airborne pathogen concentration is initially equal to 1. The air concentration then gradually increases until it reaches approximately 35.5, while the airborne pathogen concentration decreases to nearly zero.

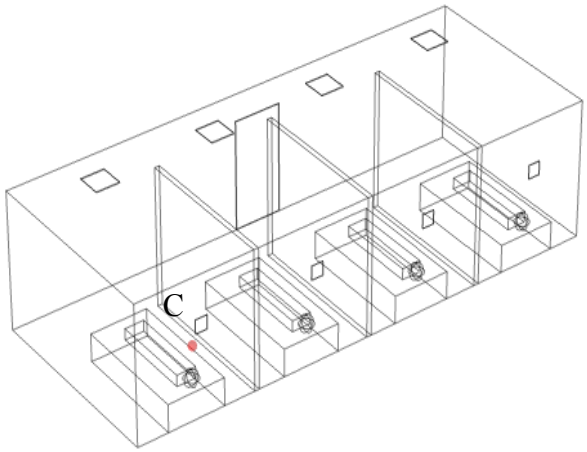

(a)

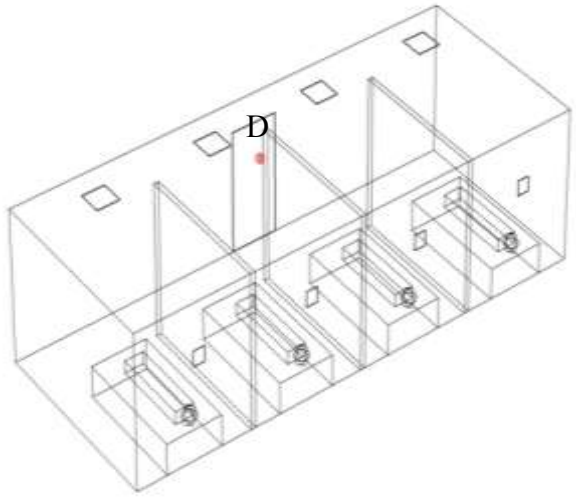

(b)

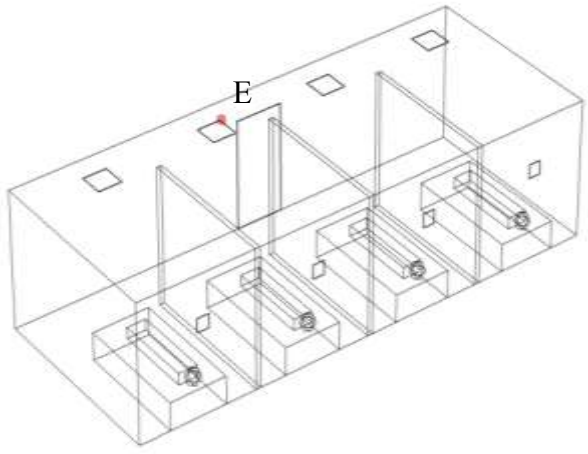

(c)

Fig. 3: Locations of points, in red, for collected computation values labeled as (a) point C, (b) point D, and (c) point E

In Figure 9, Figure10, Figure11, Figure12 and Figure 13, the molar concentration graph is shown,

depicting the scenario in which the molar mass of the airborne pathogens is equal to 5 kg/mol.

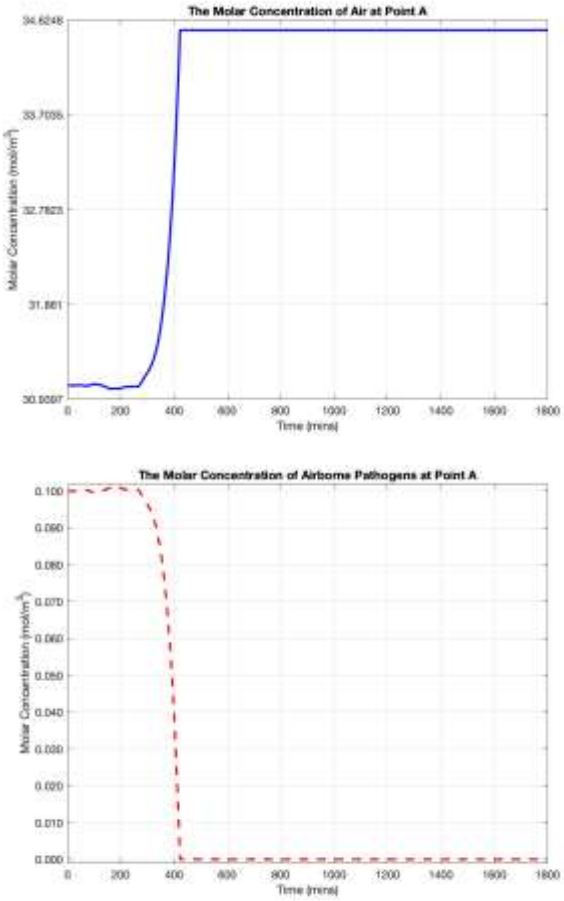

Fig. 4: Graph of molar concentration between air and airborne pathogens (molar mass = 1 kg/mol) at point A

Figure 4 and Figure 9 depict the molar concentration of air and airborne pathogens at Point A, located on the breast of the leftmost patient, with molar masses of 1 kg/mol and 5 kg/mol, respectively. We observe that the concentration of airborne pathogens with a molar mass of 1 kg/mol is initially higher than the concentration of airborne pathogens with a molar mass of 5 kg/mol. Subsequently, their concentrations drop to zero around t = 400 seconds, while the concentration of airborne pathogens with a molar mass of 5 kg/mol oscillates before also dropping to zero. Meanwhile, we observe that the molar concentration of air in both cases is initially 31 mol/m^3, increasing to approximately 34.5 mol/m^3.

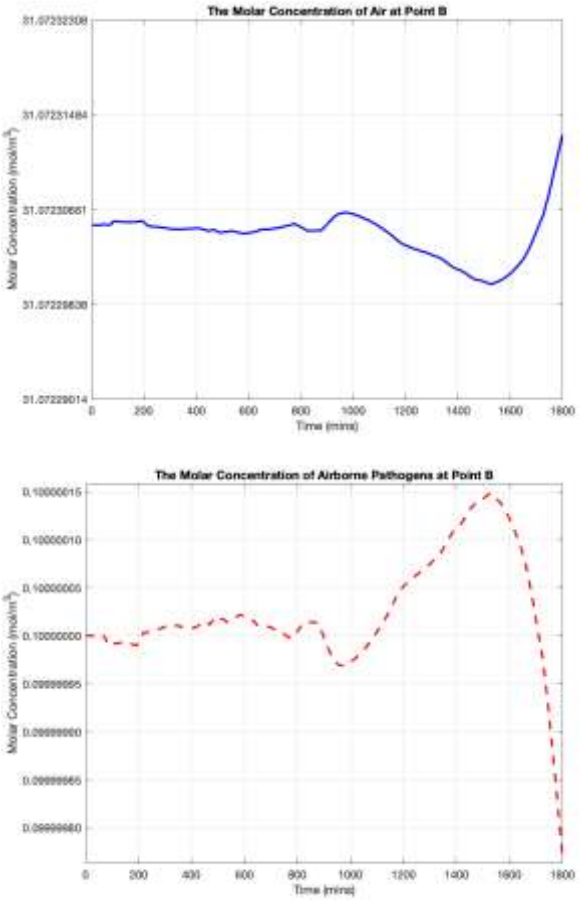

Fig. 5: Graph of molar concentration between air and airborne pathogens (molar mass = 1 kg/mol) at point B

Figure 5 and Figure 10 depict the molar concentration of air and airborne pathogens at Point B, located at the end of the bed of the leftmost patient, with molar masses of 1 kg/mol and 5 kg/mol, respectively. We observe that the molar concentration of airborne pathogens with a molar mass of 1 kg/mol is initially five times higher than the concentration of airborne pathogens with a molar mass of 5 kg/mol. The concentrations of both molar masses oscillate around their initial values up to approximately 1600 seconds in time before the concentrations of these airborne pathogens drop, indicating that the droplets are suspended in the air longer than at Point A.

Figure 6 and Figure 11 display the molar concentrations of air and airborne pathogens at Point C, situated below and near the outlet flow of the leftmost patient, with molar masses of 1kg/mol and 5 kg/mol, respectively. The results reveal similar concentration trends to those observed at Point A. However, the airborne pathogens persist in the air for approximately 600 seconds in time,

indicating a longer duration of suspension compared to Point A.

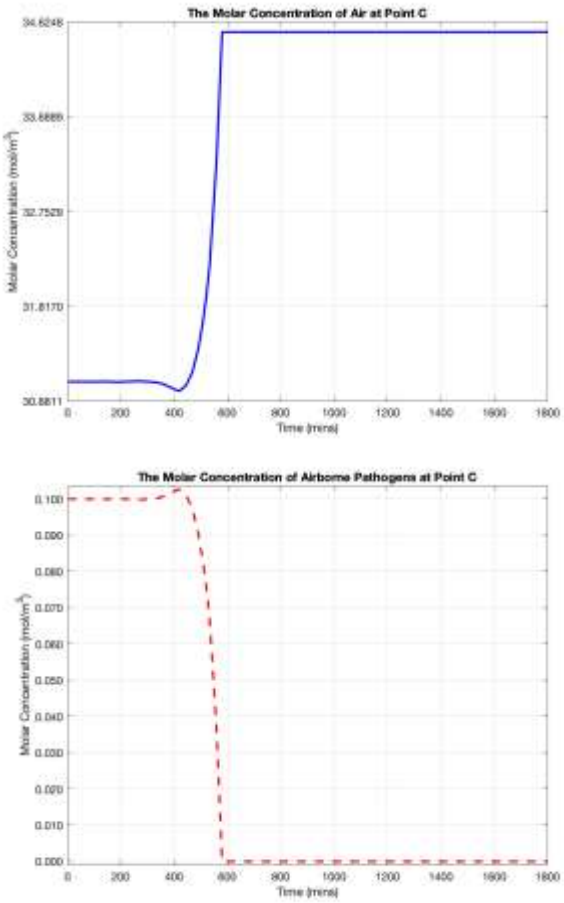

Fig. 6: Graph of molar concentration between air and airborne pathogens (molar mass = 1 kg/mol) at point C

Comparing the concentration of airborne pathogens at Point D, located at the door for entrance into the room, as shown in Figure 7 and Figure 12 for molar masses of 1 kg/mol and 5 kg/mol, respectively, reveals the following trends. For the molar mass of 1 kg/mol, the concentration slightly increases above the initial concentration value for approximately 1000 seconds and then gradually decreases below the initial concentration thereafter.

However, for the molar mass of 5 kg/mol, the concentration of airborne pathogens fluctuates and increases over time. This indicates that pathogens accumulate and persist at this point.

Next, we consider the concentration of air and airborne pathogens, with molar masses of 1 kg/mol and 5 kg/mol respectively, at Point E, located at the pure air inlet flow. The results show that for the molar mass of 1 kg/mol, the concentration of airborne pathogens fluctuates, decreasing until approximately 1000 seconds in time, and then increasing afterward. However, for the molar mass of 5 kg/mol, the concentration of airborne pathogens at this point continues to increase. This indicates that pathogens accumulate and persist at this point.

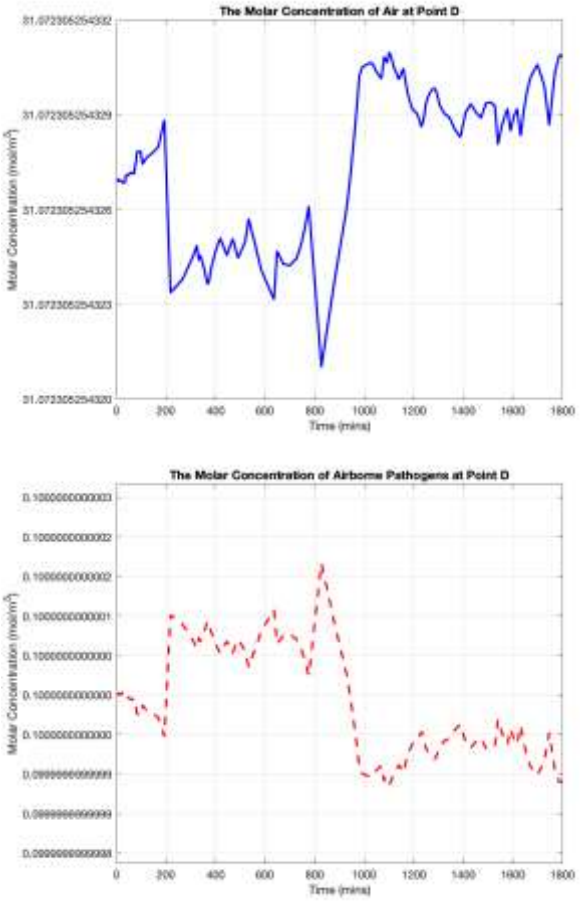

Fig 7: Graph of molar concentration between air and airborne pathogens (molar mass = 1 kg/mol) at point D

In Figure 14, the pattern of the normalized vector field presents the steady-state airflow. The air flows from each inlet on the ceiling towards the patients and exits through the outlets positioned above their heads.

Finally, Figure 15 and Figure 16 show the patterns of the normalized mass fraction gradient, at time t =1800, of airborne pathogens, simulated with a molar mass of 1 kg/mol and 5 kg/mol, respectively. We observe that the mass fraction gradient of airborne pathogens exhibits random directions and spreads throughout the entire patient's room.

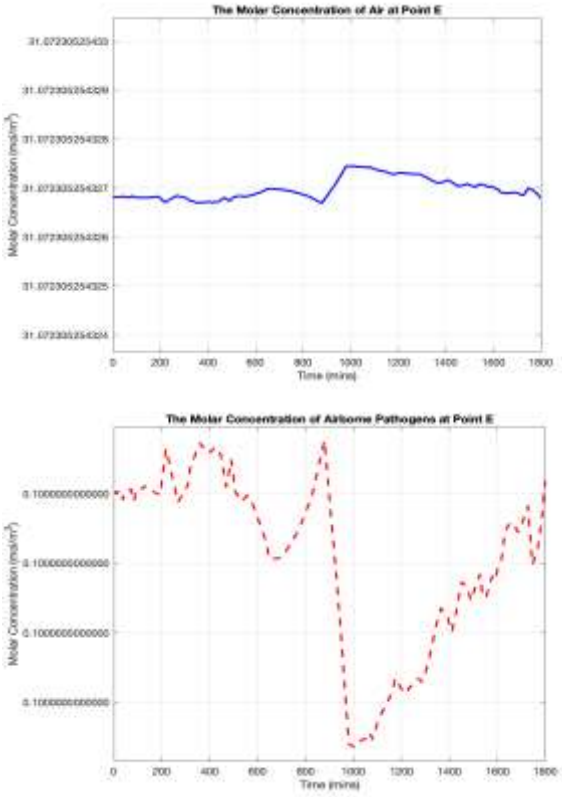

Fig. 8: Graph of molar concentration between air and airborne pathogens (molar mass = 1 kg/mol) at point E

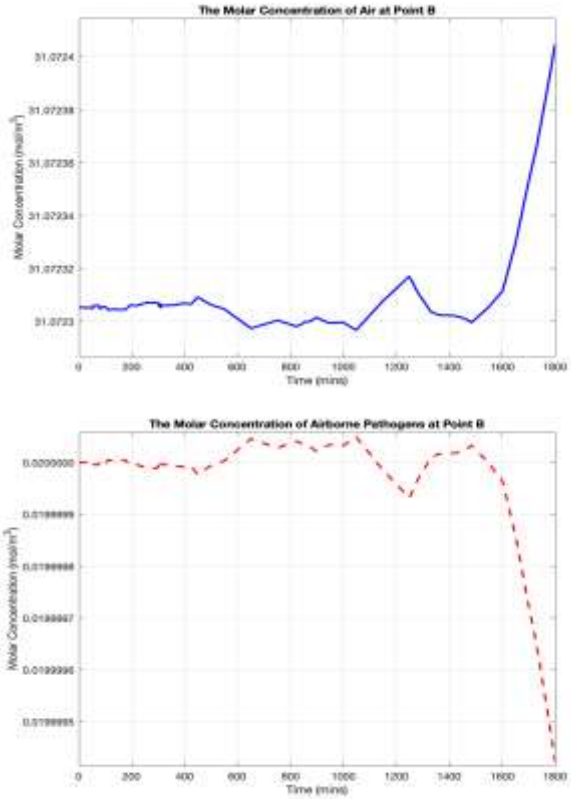

Fig. 10: Graph of molar concentration between air and airborne pathogens (molar mass = 5 kg/mol) at point B

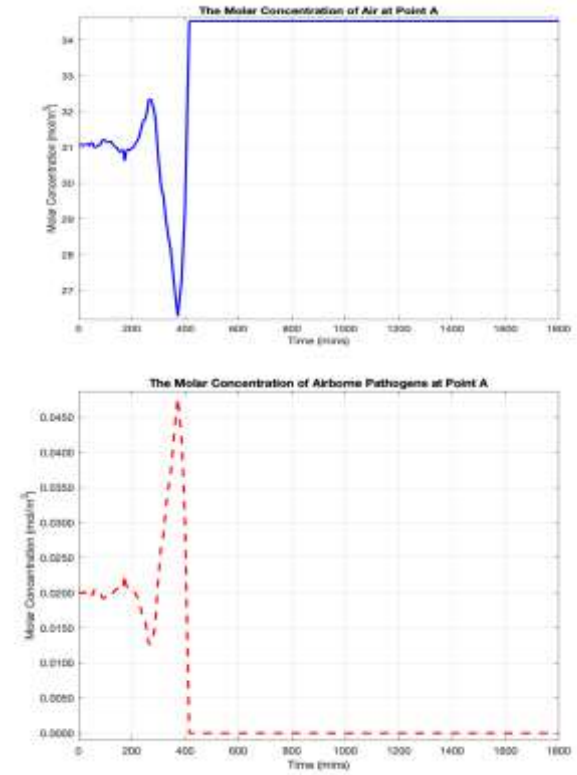

Fig. 9: Graph of molar concentration between air and airborne pathogens (molar mass = 5 kg/mol) at point A

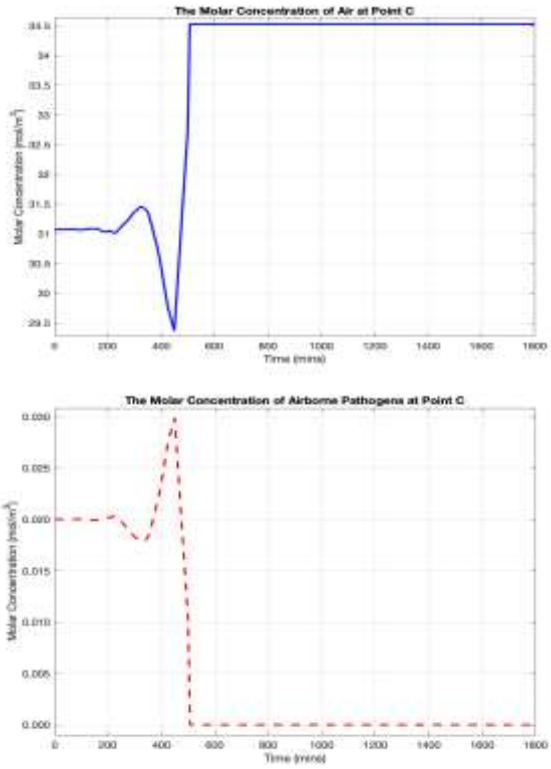

Fig. 11: Graph of molar concentration between air and airborne pathogens (molar mass = 5 kg/mol) at point C

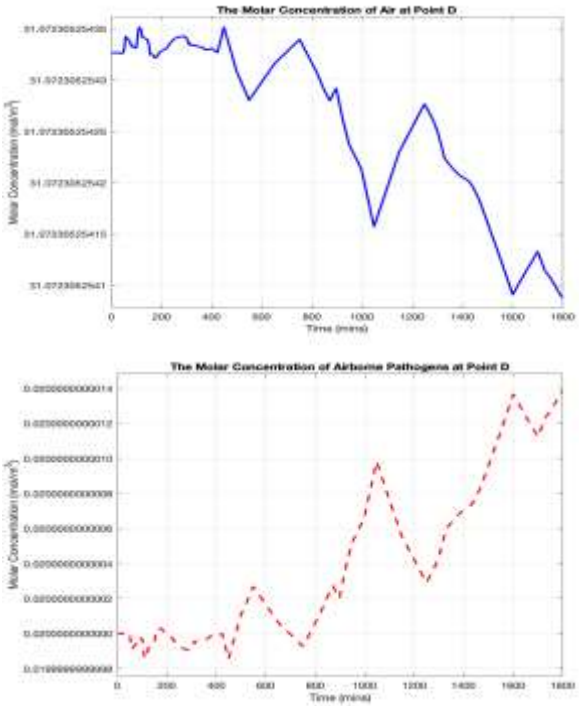

Fig. 12: Graph of molar concentration between air and airborne pathogens (molar mass = 5 kg/mol) at point D

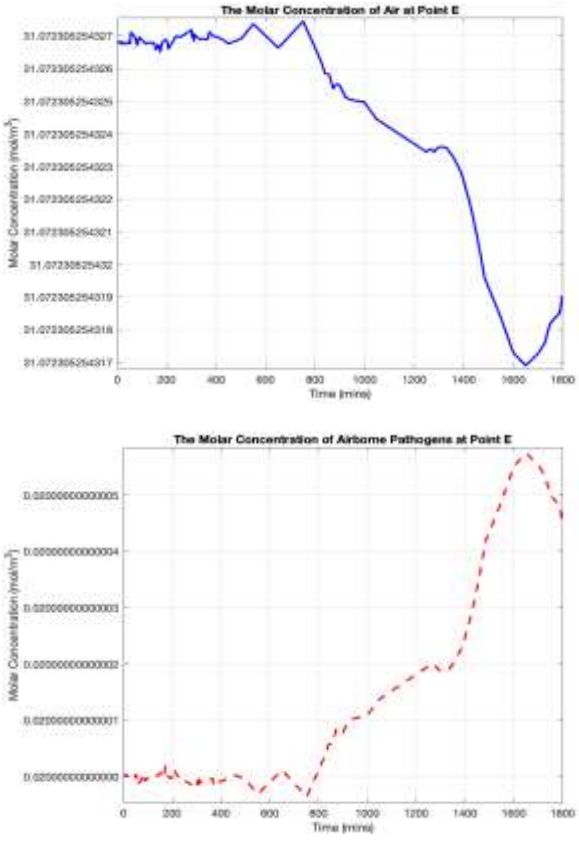

Fig. 13: Graph of molar concentration between air and airborne pathogens (molar mass = 5 kg/mol) at point E

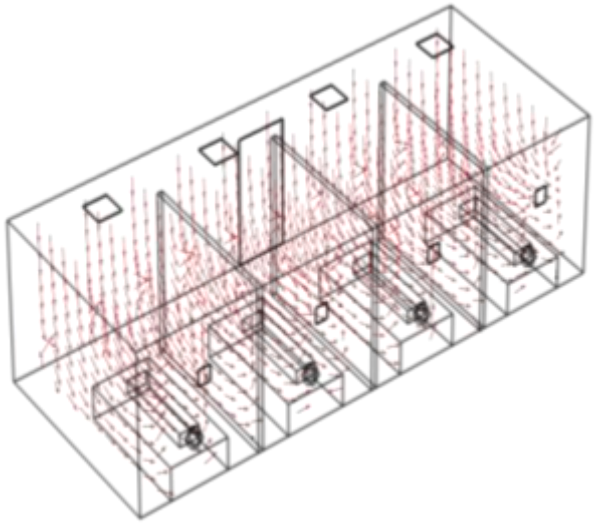

Fig. 14: Graph of the normalized vector field at the steady state of the air

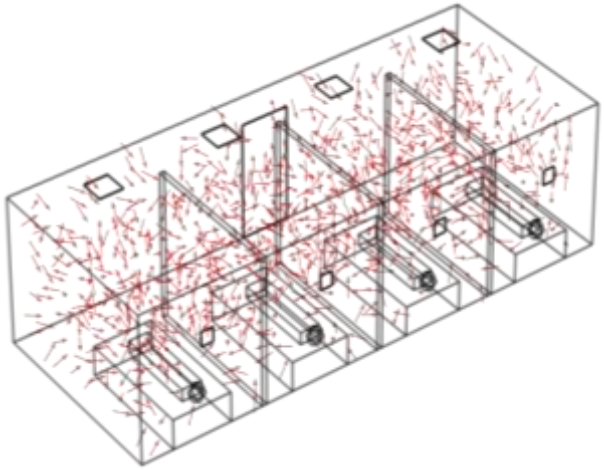

Fig. 15: Graph of the normalized mass fraction gradient of airborne pathogens, simulated with molar mass = 1 kg/mol, at time t =1800

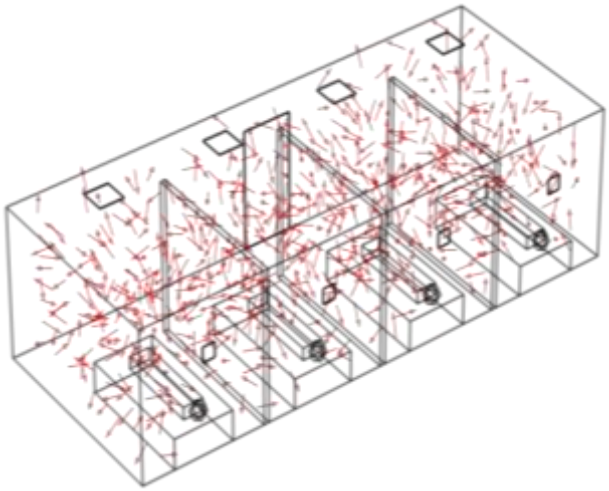

Fig. 16: Graph of the normalized mass fraction gradient of airborne pathogens, simulated with molar mass = 5 kg/mol, at time t =1800

5 Conclusion

In this work, we have examined the impact of the molar mass of airborne pathogens on the molar concentrations of air and airborne pathogens. We have observed that a greater molar mass of airborne pathogens leads to reduced dispersion of these pathogens. Specifically, our work has treated the air movement carrying the airborne virus as a particulate fluid flow which we believe was able to simulate the real scenarios more closely.

For possible future research endeavors, we can, for example, investigate how different arrangements of furniture or room designs, or different locations of the points of outlet or inlet flow would lead to different distribution patterns and how we can utilize such information to discover the optimum utility of space at minimum risk of infection. We can also study the impacts of variations in the air inflow velocity. The methodology utilized in this study can be applied to gain valuable information regarding other settings of enclosed regions under the influx of other infectious airborne pathogens.

Acknowledgement:
The author would like to thank Emeritus Professor Dr. Yongwimon Lenbury of the Centre of Excellence in Mathematics, Thailand, and Associate Professor Benchawan Wiwatanapataphee of the Department of Mathematics and Statistics, Curtin University, Australia, for their valuable suggestions and advice.

References:

[1] Shaylika Chauhan, Comprehensive review of coronavirus disease 2019 (COVID-19), *Biomed J.* 2020 Aug; 43(4): 334-340.

[2] WHO Director-General's opening remarks at the media briefing on COVID19 -March 2020, [Online]. https://www.who.int/director-general/speeches/detail/who-director-general-s-opening-remarks-at-the-media-briefing-on-covid-19---11-march-2020 (Accessed Date: February 20, 2024).

[3] Babashov, S., Predicting the Dynamics of Covid-19 Propagation in Azerbaijan based on Time Series Models. *WSEAS Transactions on Environment and Development,* Vol. 18, 2022, pp. 1036-1048, https://doi.org/10.37394/232015.2022.18.99.

[4] Makanda, G., A Mathematical Model for the Prediction of the Impact of Coronavirus(COVID19) and Social Distancing Effect, *WSEAS Transactions on Systems and Control,* Vol.15, 2020, pp. 601-613, https://doi.org/10.37394/23203.2020.15.60.

[5] Smith, C., A Dangerous New Coronavirus Complication was Discovered-and it never goes away if you get it. http://bgr.com/science/ coronavirus-symtoms complications-diabetes-onset-after-covid-19/(Last Accessed Dates: 06.03.2022)

[6] Rattanakul, C., Lenbury, Y., Khajohnsaksumeth, N. Modchang, C., Geometric Singular Perturbation Analysis of a Multiple Time-scale Model for Diabetes and COVID-19 Comorbidity, *WSEAS Transactions on Biology and Biomedicine,* Vol. 19, 2022, https://doi.org/10.37394/23208.2022.19.20.

[7] De Luca, C., Olefsky, J.M., Inflammation and Insulin Resistance, *FEBS Lett.,* Vol. 582(1), pp. 97-105. doi:10.1016/j.feslet.2007.11.057.

[8] Y Li, G M Leung, J W Tang, X Yang, C Y H Chao, J Z Lin, J W Lu, P V Nielsen, J Niu, H Qian, A C Sleigh, H-J JSu, J Sundell, T W Wong, P L Yuen, Role of ventilation in airborne transmission of infectious agents in the built environment – a multidisciplinary systematic review, *Indoor,* 2007 Feb; 17(1):2-18. doi: 10.1111/j.1600-0668.2006.00445.x.

[9] EPA, Indoor Air and Coronavirus (COVID-19), [Online]. https://www.epa.gov/coronavirus/indoor-air-and-coronavirus-covid-19 (Accessed Date: February 20, 2024).

[10] Melanie D Nembhard, D Jeff Burton, and Joel M Cohen, Ventilation use in nonmedical settings during COVID-19: Cleaning protocol, maintenance, and recommendations. *Toxicology and Industrial Health,* 2020, Vol 36(9) 644-653.

[11] Nicas, M., Nazaroff, W.W. and Hubbard, A. toward understanding the risk of secondary airborne infection: emission of respirable pathogens.*J. Occup. Environ. Hyg.s,* Vol.2, 2005, 143-154.

[12] Morawska, L., Johnson, G.R., Ristovski, Z.D., Hargreaves, M., Mengersen, K., Corbett, S., Chao, C.Y.H., Li, Y. and Katoshevski, D. Size distribution and sites of origin of droplets expelled from the human respiratory tract during expiratory activities. *J.Aerosol Sci,* Vol.40, 2009, 256-269.

[13] Yang, S., Lee, G.W.M., Chen, C.M., Wu, C.C. and Yu, K.P. The size and concentration of droplets generated by coughing in human subjects. *J.Aerosol Med.,*2007, 484-494.

[14] Wang, B., Zhang, A., Sun, J., Liu, H., Hu, J. and Xu, L. Study of SARS transmission via liquid droplets in air. *Trans.ASME,* 2005, Vol.127, 32-38A.

[15] Xie, X., Li, Y., Chwang, A.T.Y., Ho, P.L. and Seto, W.H. How far droplets can move in indoor environments – revisiting the Wells evaporation–falling curve. *Indoor,* Vol.127, 2007, 211-225.

[16] Wan, M.P. and Chao, C.Y.H. Transport characteristics of expiratory droplets and droplet nuclei in indoor environments with different ventilation air flow patterns. *J.Biomech. Eng. T-ASME,* 2007, Vol.129, 341-353.

[17] C.Chen, B.Zhao. Some questions on dispersion of human exhaled droplets in ventilation room: answers from numerical investigation. *Indoor Air,* 2010, Vol.20, 95-111.

[18] Liu, J., Chen, X., Liu, Y., Lin, J., Shen, J., Zhang, H., Yin, J., Pu, R., Ding, Y., Cao, G. (2021). Characterization of SARS-CoV-2 worldwide transmission based on evolutionary dynamics and specific viral mutations in the spike protein. Infectious Diseases of Poverty, 10(1), 89, https://doi.org/10.1186/s40249-021-00895-4.

[19] Dërmaku-Sopjani M, Sopjani M. Molecular Characterization of SARS-CoV-2. Curr Mol Med. 2021; 21(7):589-595. doi: 10.2174/1566524020999201203213037. PMID: 33272175.

[20] Unacademy. (2024). What is the molecular weight of air? [Question & Answer], [Online]. https://unacademy.com/content/question-answer/chemistry/what-is-the-molecular-weight-of-air/ (Accessed Date: February 21, 2024).

[21] Rahmstorf, L., Emanuel, K., & Ebi, K. L. (2021). Global weight of all active SARS-CoV-2 viruses is between 0.1 and 10 kilograms, [Online]. https://phys.org/news/2021-06-global-weight-sars-cov-viruses-kilograms.html (Accessed Date: February 21, 2024).

Contribution of Individual Authors to the Creation of a Scientific Article

Nathnarong Khajohnsaksumeth: problem formulation, model selection, and boundary conditions identification, choice of the numerical scheme, numerical simulations, writing, and editing.

Sources of Funding for Research Presented in a Scientific Article or Scientific Article Itself

This research has received funding support from the NSRF via the Program Management Unit for Human Resource & Institutional Development, Research and Innovation (grant number B05F640231). Also, this research is partially supported by the Centre of Excellence in Mathematics, Ministry of Higher Education, Science, Research and Innovation, Thailand (grant number RG-01-65-01-1).

Conflict of Interest

There is no conflict of interest.